Resonant extended states in driven quasiperiodic lattices: Aubry-Andre localization by design

L. Morales-Molina,[1] E. Doerner,[1] C. Danieli,[2] and S. Flach[2]

[1]*Instituto de Física, Facultad de Física, Pontificia Universidad Católica de Chile, Casilla 306, Santiago 22, Chile*

[2]*New Zealand Institute for Advanced Study, Centre for Theoretical Chemistry and Physics, Massey University, 0745 Auckland, New Zealand*

(Received 4 May 2014; published 28 October 2014)

We consider a quasiperiodic Aubry-Andre (AA) model and add a weak time-space-periodic perturbation. The undriven AA model is chosen to be well in the localized regime. The driving term controls the effective number of propagation channels. For a spatial resonance which reduces the reciprocal space dynamics to an effective one-dimensional two-leg ladder, the ac perturbation resonantly couples certain groups of localized eigenstates of the undriven AA model and turns them into extended ones. Slight detuning of the spatial and temporal frequencies off resonance returns these states into localized ones. We analyze the details of the resonant extended eigenstates using Floquet representations. In particular, we find that their size grows linearly with the system size. Initial wave packets overlap with resonant extended eigenstates and lead to ballistic spreading.

DOI: 10.1103/PhysRevA.90.043630 PACS number(s): 03.75.Hh, 03.75.Lm, 05.60.−k, 72.15.Rn

I. INTRODUCTION

More than 50 years since the publication of Anderson's seminal paper on wave-function localization in disordered lattices [1], and more than 30 years since the observation of wave-function localization in quasiperiodic lattices by Aubry and Andre [2], the field still records growing interest and activity. This is, to a large extent, due to the rapid development experienced in the field of cold atoms in optical lattices [3], and of light propagation in structured media [4]. Controllability of the system dimensions, tunability of the interaction among atoms and nonlinearity for propagating light beams, and the implementation of designed disorder potentials opens avenues for new challenges. In particular, this has allowed the study of (i) Anderson localization for noninteracting atoms [5] and light [6], and (ii) Aubry-Andre (AA) localization for noninteracting atoms [7] and light [8].

Unlike the one-dimensional Anderson model, where all eigenstates are localized irrespective of the strength of the disorder potential, the AA model of a one-dimensional quasiperiodic lattice allows for the existence of extended states as well [9]. The metal-insulator transition (MIT) separates extended states (metallic regime) from localized states (insulating regime) and is controlled by the depth of the quasiperiodic potential. Notably, the MIT for the AA model is energy independent due to a duality symmetry [2]. Extensions which include driven ac forces allow additional control over the MIT [10].

Here we address the question of whether a weak but resonant space-quasiperiodic and time-periodic perturbation can destroy AA localization. Early studies for Anderson localization with uncorrelated random potentials show that the absence of correlations allows for a finite increase of the localization length in the presence of time-periodic ac perturbations, but keeps a finite upper bound on it [11,12]. Despite a number of further publications on driven Harper models [13,14] and versions of driven AA models [15], the results are basically soft modifications of the properties of the unperturbed eigenstates in the presence of driving. We consider a time-periodic moving lattice which mimics the effect of a driving force. The amplitude of the moving lattice is taken small, but its oscillation frequency is chosen such that it resonantly couples localized states from distinct bands of the undriven AA system. At the same time, the additional spatial quasiperiodic perturbation effectively increases the dimensionality from $d = 1$ to $d = 2$ in reciprocal space. At a spatial resonance, this dynamics is reduced to an effective one-dimensional ladder topology. As a result of this resonant coupling, delocalization takes place. We use Floquet representation to extract the eigenstates of the driven system. We find that at certain resonant values of the driving frequency, groups of eigenstates completely delocalize. We study the properties of these resonant extended eigenstates, and perform wave-packet evolution tests to show that off-resonance AA localization holds, but on-resonance ballistic transport is obtained.

II. THE MODEL

Ultracold atoms in optical lattices offer an ideal benchmark for the study of Anderson localization since disordered lattices are experimentally feasible to build. For instance, a quasiperiodic lattice potential can be created by a bichromatic lattice [9,16] of the form

$$U(x) = U_1 \cos(k_1 x) + U_2 \cos(k_2 x + \phi), \tag{1}$$

where ϕ is a constant phase introduced to shift the two lattices relative to each other. Here k_1 and k_2 are the wave vectors and U_1 and U_2 are the amplitudes of the two lattice potentials (see [17] for generalizations).

Within the tight-binding approximation obtained with the limit $U_1 \gg U_2$ [9], the quantum dynamics for a particle moving in a quasiperiodic potential, given by Eq. (1), can be described by the Harper [18] or the Aubry-André (AA) model [2]. Details of the derivation of the AA model can be found, for instance, in Ref. [19]. The experimental verification of the MIT of the AA model, and therefore the realizability of the tight-binding approximation, was demonstrated in Ref. [7] for ultracold atoms. Here we consider the driven AA model,

$$i\frac{d\psi_n}{dt} = \psi_{n+1} + \psi_{n-1} + V_1 \cos(2\pi\alpha n + \delta)\psi_n + V_2 \cos(2\pi\beta n + \Omega t)\psi_n. \tag{2}$$

The first line in Eq. (2) corresponds to the undriven AA model in dimensionless units. Here ψ_n is the complex wave-function amplitude at lattice site n, V_1 is the strength of the quasiperiodic potential, α is an irrational number setting the spatial period $1/\alpha$ which is incommensurate with the lattice spacing $\Delta n \equiv 1$ (here, α will be chosen as $\alpha = \sqrt{3} - 1 \approx 0.732$), and δ is a relative phase. Note that V_1 is a certain function of $U_{1,2}$ from Eq. (1) [9]. The second line in Eq. (2) represents a time-space-periodic perturbation potential with amplitude V_2, spatial period $1/\beta$, and the ac driving frequency Ω. It can be realized with ultracold atomic gases, adding a term $U_3 \cos(k_3 x)$, $U_3 \ll U_1$, to the bichromatic lattice laser potential, together with a time-dependent variation [16] (see also [20], p. 95). Note that Eqs. (2) are invariant under shifts of α or β by any integer, and therefore their irreducible space is confined to the unit interval. Despite the time-dependent perturbation, the above equations enjoy a generalized symmetry $\beta \to -\beta$, $t \to -t$, and $\psi \to \psi^*$. For all practical computational purposes, we used a finite system size N with fixed boundary conditions $\psi_0 = \psi_{N+1} = 0$.

In the absence of ac driving, $V_2 = 0$, the system (2) is self-dual [2] and it is known to possess a MIT at the critical depth of the potential $V_1 = 2$ [2]. This is usually shown through a duality transformation. We generalize this transformation to the case of our driven model. In analogy to the procedure in [2], we define

$$\psi_n \equiv e^{i2\pi Kn} \sum_{l,m} f_{l,m} e^{i[(2\pi\alpha n+\delta)l+(2\pi\beta n+\delta)m]}. \tag{3}$$

Here, $f_{l,m}$ are the complex wave-function amplitudes in reciprocal (spatial Fourier) space with the Bloch wave number $K \in \mathbb{R}$. The indices l,m can take all integer values. They correspond to the two lattice frequencies $2\pi\alpha$ and $2\pi\beta$ of the model. So far we consider the case when the ratio α/β is irrational as well. Then Eqs. (2) turn into a two-dimensional lattice problem in reciprocal space:

$$\begin{aligned} i\frac{df_{l,m}}{dt} &= 2\cos[2\pi(\alpha l + \beta m + K)] f_{l,m} \\ &+ \frac{V_1}{2}(f_{l+1,m} + f_{l-1,m}) \\ &+ \frac{V_2}{2}[e^{i2\pi g(t)} f_{l,m-1} + e^{-i2\pi g(t)} f_{l,m+1}], \end{aligned} \tag{4}$$

where the function

$$g(t) = \Omega t - \delta \tag{5}$$

takes care of the time-dependent relative phase shifts of the two quasiperiodic potentials. The structure of the third line in Eq. (4) suggests that the second perturbation potential acts as a magnetic field. However, the total flux per plaquette in the two-dimensional reciprocal lattice $\{l,m\}$ is zero.

Let us discuss these results for $\Omega = 0$. Equation (2) is a one-dimensional Schrödinger equation (on a lattice). We could always transform it into a Bloch basis of extended plane waves. However, the consequence of that will be, in general, some nonlocal coupling between the Bloch states for irrational α and β. Instead the transformation (3) uses a basis which transforms (2) by keeping a nearest-neighbor interaction network as observed in (4). In particular, for $V_2 = 0$, the resulting network interaction is an infinite set of noninteracting one-dimensional networks, while for $V_2 \neq 0$ it becomes two dimensional. Conceptually, this is close to recent advances in emulating three-dimensional Anderson MIT using quantum kicked rotors with several additional temporal frequencies [21].

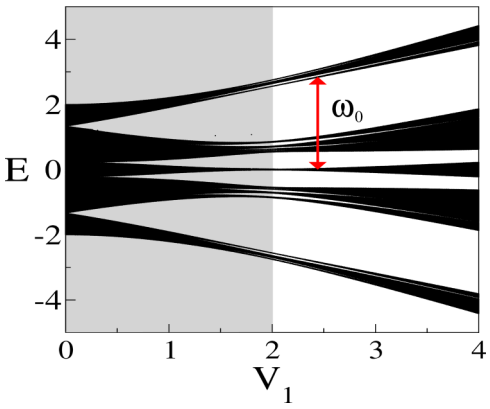

FIG. 1. (Color online) Energy spectrum E vs V_1 of the undriven Aubry-Andre model ($V_2 = 0$) with $\alpha = \sqrt{3} - 1$. The shadowed region indicates the metallic regime for $V_1 < 2$. The arrow indicates the separation between edge and center bands for $V_1 = 2.5$ within the insulating regime.

For $V_2 = 0$, the two-dimensional lattice equations (4) decouple into independent and equivalent one-dimensional ones. These chains are identical with the unperturbed Aubry-Andre case in real space (2) and exhibit a MIT at the critical value $V_1 = 2$. With the ansatz $\psi_n(t) = e^{-iEt}\phi_n$, we solve the corresponding eigenvalue problem for the eigenenergies E. Figure 1 shows the spectrum of energy E as a function of V_1. A well-defined hierarchy of gaps and subgaps appears in the spectrum between different eigenenergies, due to its topological structure (for all $V_1 \neq 0$, the spectrum is a Cantor set [22,23]). However, the nature of the corresponding eigenmodes depends on V_1, since for $V_1 > 2$ all the eigenstates are localized, whereas for $V_1 < 2$ they are extended. This means that any initially localized wave packet for $V_1 > 2$ will remain localized at all times.

III. DRIVEN LATTICE RESONANCES

Spatial resonances happen for $V_2 \neq 0$ but with a commensurate ratio of the two spatial frequencies $\alpha/\beta = p/q$, with $\{p,q\}$ integers. Then the transformation (3) extends only over q-independent integers $m = 0,1,2,\ldots,q-1$, turning the two-dimensional lattice (4) into a one-dimensional ladder with q legs. The boundary conditions between the first and the qth leg are defined by the second integer p.

Let us add a weak perturbation potential $V_2 = 0.25$ for the case $V_1 = 2.5$, where the eigenstates of the undriven system are localized. We hunt for a resonant coupling of the eigenstates of the undriven case through the ac driving. Therefore the driving frequency Ω should take values of the order of the gaps of the spectrum of the undriven case in Fig. 1.

Due to the time-periodic forcing, it is convenient to use the Floquet formalism. The wave function is expanded in terms of Floquet states $u_n(t) = e^{-i\epsilon t}\phi_n(t)$, with $\phi(t+T)_n = \phi_n(t)$,

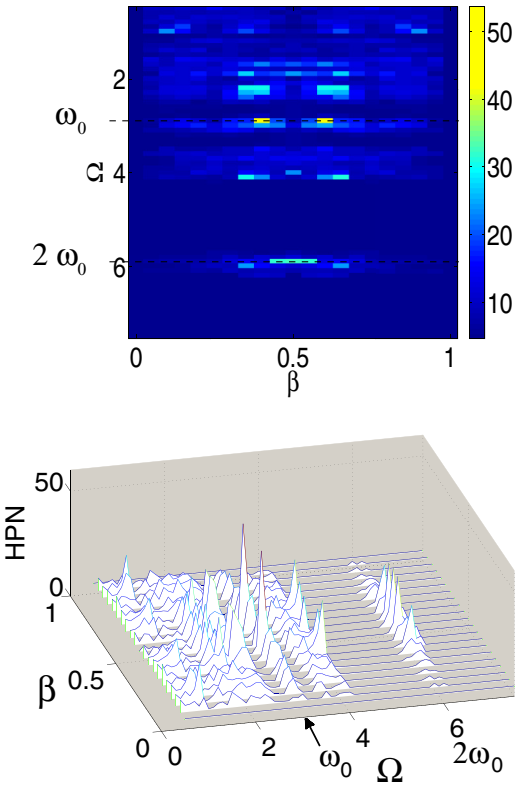

FIG. 2. (Color online) Top: Density plot of highest participation number HPN vs Ω and β. Dashed lines indicate the resonances $\Omega = \omega_0 = 2.9$ and $\Omega = 2\omega_0 = 5.8$. Bottom: Same in a three-dimensional plot, with good visibility of the strong resonance at $\beta \approx 0.37$. Here $V_1 = 2.5$, $V_2 = 0.25$, $\alpha = \sqrt{3} - 1$, and $N = 200$.

where $T = 2\pi/\Omega$ (see also [24] for details). To determine the degree of (de)localization of Floquet states, we compute the participation number [25,26]

$$PN = \frac{\sum_n |u_n|^2}{\sum_n |u_n|^4}, \tag{6}$$

with the lower bound $PN = 1$ which accounts for maximal localization, and the upper bound $PN = N$ corresponding to an extended state with constant amplitude (here N is the number of lattice sites). Any localized eigenstate will produce a finite PN which does not scale with the system size $N \gg PN$. Extended eigenstates have fluctuating amplitudes, and their PN is always less than N, strictly speaking with no lower bound on the ratio PN/N. However, their distinct feature is that PN scales linearly with N. For each parameter set $\{\beta,\Omega\}$, we find all Floquet eigenstates, compute PN for each of them, and identify the highest value HPN. Figure 2 shows the intensity plot of HPN as a function of β and Ω. While even the states with the largest spatial extend stay very localized for almost all parameter values, we find a strong resonant spot at $\beta \approx 0.37$ and $\Omega \approx 2.9$, and its symmetry related partner point at $\beta \approx 0.63$. Weaker spots are observed at $\Omega \approx 2.4,4,5.8$.

At the main resonance, β corresponds approximately to $\alpha/2$. Therefore, the two-dimensional lattice in reciprocal space (4) is reduced to a two-leg ladder. The resonance frequency $\Omega = 2.9$ fits very well the distance between the

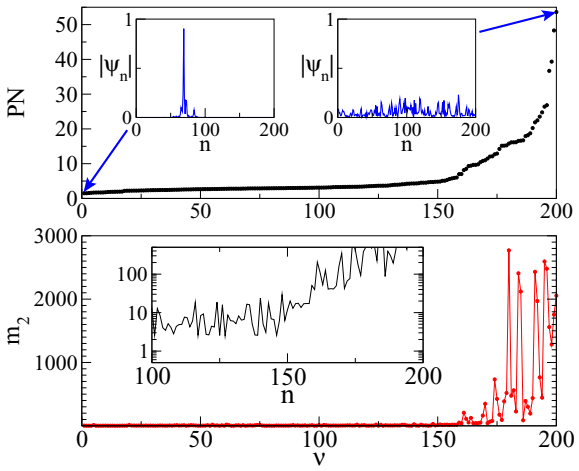

FIG. 3. (Color online) Upper panel: Ordered values of PN of the Floquet states vs Floquet state number ν. Insets: The absolute value of the wave function vs lattice site n for the state with smallest and largest PN. Lower panel: Same for the second moment m_2, with the sorting index from the upper panel. Inset: Enlargement of the region around the number 150 for a logarithmic scale. Here $V_2 = V_1/10 = 0.25$, $\alpha = \sqrt{3} - 1$, $\beta = 0.37$, $\Omega = 2.9$, and $N = 200$.

edge and center bands in Fig. 1. To make sure that the observed resonance is indeed due to extended states, we plot in Fig. 3 the participation numbers PN for all Floquet eigenstates of a system with size $N = 200$ sorted according to their increasing value. In addition, we also plot their second moments,

$$m_2 = \sum_n (n - \langle n_0 \rangle)^2 |u_n|^2, \tag{7}$$

where $\langle n_0 \rangle = \sum_n n|u_n|^2$ is the first moment of the wave packet. Note that we do not reorder the second moments, but plot them using the sorting principle for the participation numbers. We find that states with increasing size are detected using both measures. In the inset of the upper panel in Fig. 3, we show the wave function of the state with the smallest PN and the largest HPN. While the former one is strongly localized, the state with HPN is clearly delocalized over the whole system.

If the observed resonance is leading to complete delocalization in an infinite system, the HPN should scale linearly with the system size N of a finite lattice. We test this prediction and show in Fig. 4 that it is indeed correct. Therefore, the observed resonance at $\Omega = 2.9$ and $\beta = 0.37$ generates extended eigenstates.

In the presence of stronger driving, the observed resonances are expected to broaden. We test this prediction repeating the calculation in Fig. 2 while doubling the strength of the driving potential $V_2 = 0.5$. The outcome is shown in Fig. 5 and confirms our expectations.

IV. WAVE-PACKET SPREADING

Another consequence of the generation of delocalized extended eigenstates is that an initially localized wave packet will spread if at least a part of it has nonzero overlap with extended eigenstates. We perform an integration of the

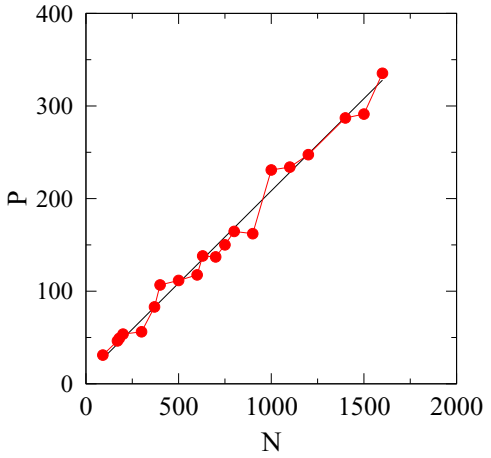

FIG. 4. (Color online) Highest participation number HPN as a function of the system size N at resonance $\beta = 0.37$, $\Omega = 2.9$. Other parameters are $V_1 = 2.5$, $V_2 = 0.25$, $\alpha = \sqrt{3} - 1$.

time-dependent equation (2) using a modified $SBAB_2$ symplectic integrator [27] with initial condition $\psi_{N/2}(t = 0) = 1$ and $\psi_{n\neq N/2}(t = 0) = 0$. For the Floquet eigenvalue problem on an infinite lattice, the eigenvalues and eigenvectors are insensitive to the value of the relative phase δ [see Eq. (2)], which essentially shifts the potential relative to the lattice. The overlap of a given initial state with Floquet eigenstates, however, does depend in general on the location of the initial state, or equivalently on the value of δ. We perform short runs for the resonance case $\beta = 0.37, \Omega = 2.9$ up to $t = 10^3$ with system size $N = 2^8$, and measure the second moment m_2 as a function of δ (Fig. 6). Note that in all cases the system size was large enough so that the wave packet did not reach the system boundaries. As expected, we find strong fluctuations due to varying overlap. We choose $\delta \approx 1.225$ and perform long-time runs up to $t = 10^5$ with system size up to $N = 2^{15}$ for several values of $V_2 = 0.25, 0.275, 0.325, 0.5$. We plot the time dependence of $\log_{10} m_2(t)$ versus $\log_{10} t$ in Fig. 7. For $V_2 = 0.5$ (blue top line), we observe ballistic spreading $m_2 \sim t^2$ over three decades in time. When lowering V_2, the onset of ballistic spreading is postponed and preceded by an intermediate spreading regime which resembles normal

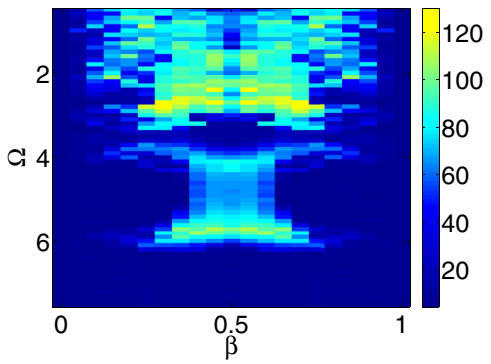

FIG. 5. (Color online) Density plot of the highest participation number HPN vs Ω and β. Here $V_1 = 2.5$, $V_2 = 0.5$, $\alpha = \sqrt{3} - 1$, and $N = 200$.

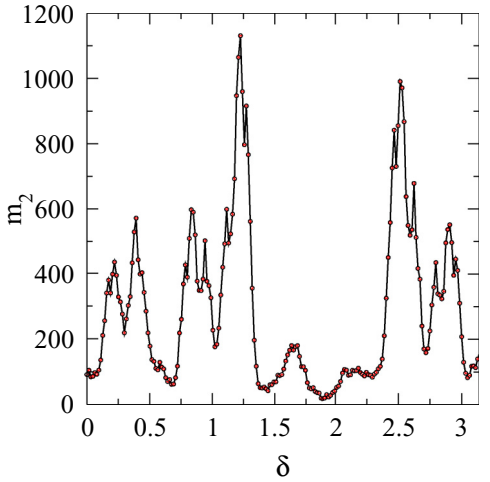

FIG. 6. (Color online) Second moment m_2 of $|\psi_n(t = 10^3)|^2$ as a function of δ for a single-site excitation at resonance $\beta = 0.37$, $\Omega = 2.9$. Other parameters are $V_1 = 2.5$, $V_2 = 0.25$, $\alpha = \sqrt{3} - 1$, $N = 2^8$.

diffusion $m_2 \sim t$. This is a typical feature of approaching a MIT, since at the critical point (here $V_2 \to 0$) the system transits into a localized insulating regime. The inset in Fig. 7 shows that the density distribution for $t = 10^5$ and $V_2 = 0.25$ has a clearly visible extended part (originating from the overlap with extended eigenstates). A test run off resonance with $\Omega = 2.6$ shows no signature of spreading, a small second moment which is constant on average, and a highly localized wave-function density at the final integration time in Fig. 7.

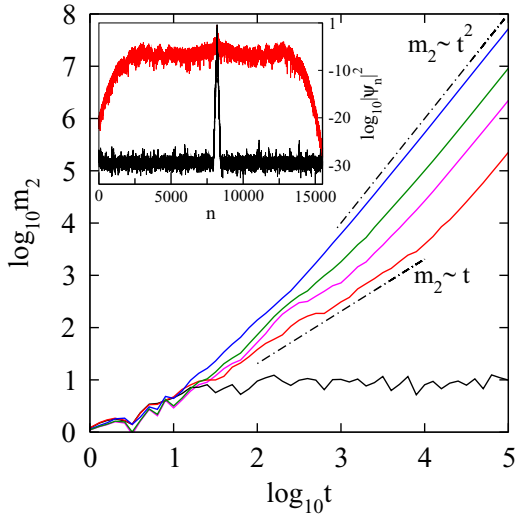

FIG. 7. (Color online) $\log_{10} m_2$ vs $\log_{10} t$. From top to bottom: $\Omega = 2.9$ and $V_2 = 0.5$ (blue), $V_2 = 0.325$ (green), $V_2 = 0.275$ (magenta), $V_2 = 0.25$ (red), and $\Omega = 2.6$ and $V_2 = 0.25$ (black, off resonance). The dash-dotted lines indicate normal diffusion $m_2 \sim t$ and ballistic spreading $m_2 \sim t^2$. In all cases, $\beta = 0.37$, $V_1 = 2.5$, $\alpha = \sqrt{3} - 1$, $\delta \approx 1.225$, $N = 2^{15}$. Inset: Density distribution of the wave function at the final time of integration for $V_2 = 0.25$. Red extended curve: $\Omega = 2.9$ (on resonance); black localized curve: $\Omega = 2.6$ (off resonance). Other parameters as in the main figure.

V. CONCLUDING REMARKS

We have studied the Aubry-Andre system in the presence of a weak driving force. The driving force is introduced upon superimposing a moving time-periodic lattice over a stationary quasiperiodic potential. The undriven AA model is chosen to be well in the insulating regime. For a spatial resonance which reduces the reciprocal space dynamics to an effective one-dimensional two-leg ladder case, the ac perturbation resonantly couples groups of localized eigenstates of the undriven AA model and turns them into extended ones. Slight detuning of the spatial and temporal frequencies off resonance returns these states into the family of localized ones. Initial wave packets overlap with resonant extended eigenstates and lead to ballistic spreading. Therefore, the proposed ac perturbation can be used as a simple and elegant method to control the degree of localization of wave packets in quasiperiodic lattices.

ACKNOWLEDGMENTS

We thank Xiaoquan Yu for help with the $SBAB_2$ code. L.M.-M. acknowledges financial support from the FONDECYT Projects No. 1110671, No. 1130705, and No. 1141223.

[1] P. W. Anderson, Phys. Rev. **109**, 1492 (1958).
[2] S. Aubry and G. André, Ann. Israel Phys. Soc. **3**, 133 (1980).
[3] I. Bloch, J. Dalibard, and W. Zwerger, Rev. Mod. Phys. **80**, 885 (2008).
[4] F. Lederer, G. I. Stegeman, D. I. Christodoulides, G. Assanto, M. Segev, and Y. Silberberg, Phys. Rep. **463**, 1 (2008).
[5] J. Billy, V. Josse, Z. Zuo, A. Bernard, B. Hambrecht, P. Lugan, D. Clement, L. Sanchez-Palencia, P. Bouyer, and A. Aspect, Nature (London) **453**, 891 (2008).
[6] T. Schwartz, G. Bartal, S. Fishman, and M. Segev, Nature (London) **446**, 52 (2007); Y. Lahini, A. Avidan, F. Pozzi, M. Sorel, R. Morandotti, D. N. Christodoulides, and Y. Silberberg, Phys. Rev. Lett. **100**, 013906 (2008).
[7] G. Roati, C. D'Errico, L. Fallani, M. Fattori, C. Fort, M. Zaccanti, G. Modugno, M. Modugno, and M. Inguscio, Nature (London) **453**, 895 (2008).
[8] Y. Lahini, R. Pugatch, F. Pozzi, M. Sorel, R. Morandotti, N. Davidson, and Y. Silberberg, Phys. Rev. Lett. **103**, 013901 (2009).
[9] M. Modugno, New J. Phys **11**, 033023 (2009).
[10] K. Drese and M. Holthaus, Phys. Rev. Lett. **78**, 2932 (1997).
[11] H. Yamada and K. S. Ikeda, Phys. Rev E **59**, 5214 (1999).
[12] D. F. Martinez and R. A. Molina, Phys. Rev. B **73**, 073104 (2006).
[13] L. Hufnagel, M. Weiss, A. Iomin, R. Ketzmerick, S. Fishman, and T. Geisel, Phys. Rev. B **62**, 15348 (2000).
[14] R. Lima and D. Shepelyansky, Phys. Rev. Lett. **67**, 1377 (1991).
[15] A. R. Kolovsky and G. Mantica, Phys. Rev. B **86**, 054306 (2012).
[16] G. Ritt, C. Geckeler, T. Salger, G. Cennini, and M. Weitz, Phys. Rev. A **74**, 063622 (2006).
[17] E. I. Dinaburg and Ya. G. Sinai, Func. Anal. Appl. **9**, 279 (1975).
[18] P. G. Harper, Proc. Phys. Soc. A **68**, 874 (1955).
[19] G. Roux, T. Barthel, I. P. McCulloch, C. Kollath, U. Schollwöck, and T. Giamarchi, Phys. Rev. A **78**, 023628 (2008).
[20] S. Denisov, S. Flach, and P. Hänggi, Phys. Rep. **538**, 77 (2014).
[21] J. Chabe, G. Lemarie, B. Gremaud, D. Delande, P. Szriftgiser, and J.-C. Garreau, Phys. Rev. Lett. **101**, 255702 (2008).
[22] A. Avila and S. Jitomirskaya, Ann. Math. **170**, 303 (2009).
[23] J. Bellissard and B. Simon, J. Func. Anal. **48**, 408 (1982).
[24] S. Denisov, L. Morales-Molina, and S. Flach, Europhys. Lett. **79**, 10007 (2007); S. Denisov, L. Morales-Molina, S. Flach, and P. Hänggi, Phys. Rev. A **75**, 063424 (2007).
[25] F. Wegner, Z. Phys. B **36**, 209 (1980).
[26] B. Kramer and A. MacKinnon, Rep. Prog. Phys. **56**, 1469 (1993).
[27] H. Yoshida, Phys. Lett. A **150**, 262 (1990); Cel. Mech. Dyn. Astr. **56**, 27 (1993); J. Laskar and P. Robutel, *ibid.* **80**, 39 (2001).